Gate imperfection in the quantum random-walk search algorithm



2006 J. Phys. A: Math. Gen. 39 9309

(http://iopscience.iop.org/0305-4470/39/29/021)

INSTITUTE OF PHYSICS PUBLISHING JOURNAL OF PHYSICS A: MATHEMATICAL AND GENERAL

J. Phys. A: Math. Gen. **39** (2006) 9309–9319 doi:10.1088/0305-4470/39/29/021

# Gate imperfection in the quantum random-walk search algorithm

**Yun Li, Lei Ma and Jie Zhou**

Department of Physics, East China Normal University, Shanghai 200062, People's Republic of China

E-mail: lma@phy.ecnu.edu.cn

Received 7 September 2005, in final form 20 March 2006
Published 5 July 2006
Online at stacks.iop.org/JPhysA/39/9309

**Abstract**

We study how imperfect quantum gates affect the quantum random-walk search algorithm. We find that systematic errors in phase inversions result in the reduction of the maximum probability of the marked state and lower the algorithm efficiency with an increasing degree of inaccuracy. The size of the database should be limited due to the inevitable errors. Finally, we compare the phase noise caused by such errors in the random-walk search algorithm with that in the Grover search algorithm.

PACS numbers: 03.67.Lx, 89.70.+c

## 1. Introduction

It is well known that for certain computational tasks, quantum algorithms are more efficient than classical ones. One such example is the Grover search algorithm [1], which has been successfully demonstrated in CQED [2] and liquid NMR bulk quantum computers on several qubits [3, 4]. The possibility of realizing such an algorithm with a coherent atomic system has also been studied [5]. Another example is the quantum random-walk (QRW) search algorithm, which has nearly the same speed as the Grover search algorithm. As the quantum counterpart of classical random walk, the QRW has been well studied [9–15], and several algorithms based on the QRW have been introduced in recent years [6–8].

Due to inevitable quantum state decoherence and gate inaccuracy, a variety of errors may be introduced in the process of computation [16]. They will accumulate throughout the computation and make long computation unreliable. Fortunately, studies of quantum error correction show that in principle an arbitrarily long quantum computation can be performed reliably if the average probability of error per quantum gate is less than a certain threshold [17]. Recently, decoherence in the QRW has been considered [18, 19]. These studies show that some properties of the QRW are highly sensitive to decoherent events, e.g. the quadratic increase of the variance will be suppressed because of decoherence. It has also been noted that

  

a small amount of decoherence can be tolerated by the QRW and can actually help some aspects of the QRW's performance. However, the mechanism of gate inaccuracy in the QRW acting on the search algorithm is seldom studied. Different types of errors occur with different rates and will affect the efficiencies of the algorithm differently. Therefore, a good understanding of a variety of errors can help us implement the algorithm more efficiently.

In this paper we study how imperfect quantum gates affect the QRW search algorithm presented in [6] without decoherence and error corrections. We assume that the Grover diffusion operator used in the algorithm is not applied perfectly, i.e. there is a noise in phase inversions. As is well known, any phase inversion operation is imperfect, so there is an uncertainty. We study the effect of such *phase noise* and demonstrate how it acts on the result of the search algorithm. The corresponding work of gate imperfection in the Grover search algorithm has been studied [20, 21]. Nevertheless, our studies show notable differences, as well as similarities, in the response of the two algorithms to noise.

The paper is organized as follows. Section 2 is a brief overview of the discrete-time quantum random walk search algorithm. Section 3 gives a model of an imperfect quantum gate in the above algorithm, and demonstrates the effect of such imperfection acting on the algorithm. Section 4 shows the numerical calculations, and compares the phase noise in the QRW search algorithm with that in the Grover search algorithm. Conclusions are presented in section 5.

## 2. Random-walk search algorithm in the absence of noise

The discrete-time quantum random walk search algorithm is realized by repeatedly applying a unitary evolution operator $U'$ on a Hilbert space $H^C \otimes H^S$ [6]. Here, $H^C$ is a $n$-dimensional Hilbert space associated with a quantum coin, and $H^S$ is a $2^n$-dimensional Hilbert space associated with the nodes of the graph. The operator $U'$ is written as follows,

$$U' = SC, \tag{1}$$

where $S$ is a permutation matrix which performs a controlled shift based on the state of the coin space. The operator $S$ moves the walker from one state to another by flipping a single qubit (e.g. $|001101\rangle$ to $|011101\rangle$), i.e. the walk composes a hypercube of dimension $n$. It can be written in the form [6]

$$S = \sum_{d=0}^{n-1} \sum_{\vec{x}} |d, \vec{x} \oplus \vec{e_d}\rangle\langle d, \vec{x}|. \tag{2}$$

The operator $C$ is a unitary matrix corresponding to flipping the quantum coin, and it can be written as

$$C = C_0 \otimes I_n + (C_1 - C_0) \otimes |\vec{0}\rangle\langle\vec{0}|. \tag{3}$$

Here $|\vec{0}\rangle$ is the marked state, $C_0$ and $C_1$ are $n \times n$ unitary operators acting on the coin space $H^C$. In order to achieve a search, different coins should be applied to different nodes. $C_0$ is the coin for unmarked node, and $C_1$ is the coin for marked node.

A frequent choice of $C_0$ is the Grover diffusion operator which is given by

$$C_0 = -I_n + 2|s^C\rangle\langle s^C|, \tag{4}$$

where $|s^C\rangle$ is the equal superposition over all $n$ directions, i.e. $|s^C\rangle = 1/\sqrt{n}\sum_{d=1}^{n}|d\rangle$. The coin $C_1$ can be chosen, for simplicity, as $C_1 = -I_n$. The initial state $|\psi_0\rangle$ is supposed to be the direct product of the superposition of all $2^n$-node and their $n$-directions. It can be written

as follows:

$$|\psi_0\rangle = \frac{1}{\sqrt{2^n \times n}}(1, 1, \ldots, 1)^T.$$

With the above selections, we apply the operator $U'$ to the initial state $|\psi_0\rangle$ repeatedly. After $t_f$ iterations where

$$t_f = \pi\sqrt{2^{n-1}}/2, \tag{5}$$

we take a measurement, and the probability of finding the target state is about $P_{\text{success}} = 1/2 - O(1/n)$.

## 3. Effect of gate imperfection in the algorithm

From the above section, we observe that the discrete-time QRW search algorithm essentially consists of two steps in one iteration: (1) flipping the coin by using the operator $C$ given in equation (3); (2) applying a shift operation by using the operator $S$ given in equation (2). In this paper, we focus on the imperfections in the Grover diffusion operator ($C_0$), and the other operators, i.e. $C_1$ and $S$, are assumed to be ideal. We start with introducing a noise in phase inversions in the Grover diffusion operator. A similar model has been adopted in [20, 21] for the Grover search algorithm. The operator $\widetilde{C}_0$ can be rewritten as

$$\widetilde{C}_0 = -I_n + (1 - \mathrm{e}^{\mathrm{i}\theta})|s^C\rangle\langle s^C|, \tag{6}$$

where $\theta = \pi + \delta$, and $\delta$ is a small constant denoting the phase noise (assume that $\delta \geqslant 0$). In this paper, we will use primed quantities to denote the QRW search algorithm in the presence of a marked node and a tilde to denote the QRW search algorithm in the presence of phase noise. For instance, $U$ is the evolution operator of a QRW with no marked node and no phase noise while $\widetilde{U}'$ is the evolution operator with a marked node and phase noise.

When $\delta = 0$, we recover the ideal QRW search algorithm without noise. In such a case, the initial state $|\psi_0\rangle$ and the final state $|\psi_1\rangle$ can be well approximated by linear combinations of two eigenvectors of $U'$, which can be written as

$$|\psi_0\rangle \simeq \frac{1}{\sqrt{2}}(|\omega_0'\rangle + |-\omega_0'\rangle), \tag{7}$$

$$|\psi_1\rangle \simeq \frac{1}{\mathrm{i}\sqrt{2}}(|\omega_0'\rangle - |-\omega_0'\rangle), \tag{8}$$

where $|\omega_0'\rangle$ and $|-\omega_0'\rangle$ are the eigenvectors of $U'$ whose eigenvalues are $\mathrm{e}^{\mathrm{i}\omega_0'}$ and $\mathrm{e}^{-\mathrm{i}\omega_0'}$ respectively. $|\psi_1\rangle$ is the state in which there is a high probability of finding the marked state $|\vec{0}\rangle$. By applying $U'$ repeatedly to the initial state $|\psi_0\rangle$, we will approach $|\psi_1\rangle$ after approximately $t_f$ iterations. Since $\omega_0' \approx -1/(c\sqrt{2^{n-1}})$ [6], the optimal number of iterations, $t_f$, will be specified approximately by equation (5). However, if $\delta$ is nonzero, we will obtain a different evolution operator $\widetilde{U}'$. It might be difficult to approach the final state by applying $\widetilde{U}'$ to $|\psi_0\rangle$ for several reasons:

(i) Due to the presence of the phase noise, the eigenvalues of $\widetilde{U}'$ will change from $\mathrm{e}^{\pm\mathrm{i}\omega_0'}$ to $\mathrm{e}^{\mathrm{i}\widetilde{\omega}_0'}$ and $\mathrm{e}^{\mathrm{i}\widetilde{\omega}_1'}$. The corresponding eigenvectors, $|\widetilde{\omega}_0'\rangle$ and $|\widetilde{\omega}_1'\rangle$, are no longer complex conjugates of one another because $\widetilde{U}'$ is not real. Thus, the state $|\psi_0\rangle$ cannot be converted into $|\psi_1\rangle$ after $t_f$ iterations.

(ii) The states $|\psi_0\rangle$ and $|\psi_1\rangle$ can no longer be written as linear combinations of $|\widetilde{\omega}_0'\rangle$ and $|\widetilde{\omega}_1'\rangle$ as equations (7) and (8). This is because the subspace spanned by $|\psi_0'\rangle$ and $|\psi_1'\rangle$ is not the same as that spanned by $|\widetilde{\omega}_0'\rangle$ and $|\widetilde{\omega}_1'\rangle$.

(iii) Even if $|\psi_0\rangle$ and $|\psi_1\rangle$ span the same subspace as $|\widetilde{\omega}'_0\rangle$ and $|\widetilde{\omega}'_1\rangle$ (when the noise is sufficiently small), the linear coefficient may be different from equations (7) and (8). Then it may be impossible to perform a complete rotation from $|\psi_0\rangle$ to $|\psi_1\rangle$.

Next we will examine the eigenvalues of $\widetilde{U}'$. However, it is difficult to specify these eigenvalues completely, because the coin used on the marked node is different from the others in order to locate the target state. So we start with an unperturbed operator $\widetilde{U}$, i.e. the evolution operator of a QRW with no marked node,

$$\widetilde{U} = S\widetilde{C}, \tag{9}$$

where $S$ can be described by equation (2) and the operator $\widetilde{C}$ is given as follows,

$$\widetilde{C} = \widetilde{C}_0 \otimes I_n. \tag{10}$$

In this case, every node on the hypercube is equivalent, and the coin space $H^C$ is separable from the node space $H^S$. Then the eigenstates of $\widetilde{U}$ are simply the tensor product of the eigenstates of an operator $C_{\vec{k}}$ on the coin space and the Fourier modes of the hypercube labelled by $n$-bit strings $\vec{k} = (k_1, k_2, \ldots, k_n)$. As in [22], we can obtain the *non-trivial* eigenvalues of $\widetilde{U}$,

$$\widetilde{\lambda} = \begin{cases} -\mathrm{e}^{\mathrm{i}\theta}, & k = 0 \\ \frac{1}{2}(1-\mathrm{e}^{\mathrm{i}\theta}) - (1-\mathrm{e}^{\mathrm{i}\theta})\frac{k}{n} & \\ \quad \mp\frac{1}{2}\sqrt{(1-\mathrm{e}^{\mathrm{i}\theta})^2\frac{(n-k)^2}{n^2} + 4\,\mathrm{e}^{\mathrm{i}\theta}}, & k = 1, \ldots, n-1 \\ \mathrm{e}^{\mathrm{i}\theta}, & k = n \end{cases} \tag{11}$$

where $\theta = \pi + \delta$. Due to the phase noise $\delta$, the operator $\widetilde{U}$ is complex, and the eigenvalues are no longer conjugated, but they still stay at the unit circle of the complex plane. The corresponding *non-trivial* eigenvectors for a given $k$ can be described as

$$|\widetilde{\nu}_k\rangle = \frac{1}{\sqrt{Q}}(\underbrace{x, x, \ldots}_{n-k}, \underbrace{y, y, \ldots}_{k}), \tag{12}$$

where $Q$ is a normalized coefficient, and $x$, $y$ satisfy the following condition

$$\frac{x}{y} = \frac{(1+\mathrm{e}^{\mathrm{i}\theta}) \pm \sqrt{(1-\mathrm{e}^{\mathrm{i}\theta})^2\frac{(n-2k)^2}{n^2} - 4(1-\mathrm{e}^{\mathrm{i}\theta}) + 4}}{2(1-\mathrm{e}^{\mathrm{i}\theta})\frac{(n-k)}{n}}$$

under $k \neq 0$ and $k \neq n$. Particularly, when $k = 0$, $|\widetilde{\nu}_k\rangle = |\psi_0\rangle$. There is a small deviation between $\widetilde{\lambda}'$ (i.e. $\mathrm{e}^{\mathrm{i}\widetilde{\omega}'_j}$, $j = 0, 1, \ldots$), the eigenvalues of $\widetilde{U}'$, and $\widetilde{\lambda}$, the eigenvalues of $\widetilde{U}$. In figure 1, we show the eigenvalue spectra of the unperturbed and perturbed matrices for $n = 8$ with the noise $\delta = 0.1$. We stress that the eigenvalues $\widetilde{\lambda}'_0$ and $\widetilde{\lambda}'_1$ are not complex-conjugate pairs, unless there is no noise. However, with the increasing of $\delta$, numerical studies show that these two eigenvalues will respectively approach $-\mathrm{e}^{\mathrm{i}\theta}$, and 1 gradually, where the former is exactly the eigenvalue of $\widetilde{U}$ for $k = 0$ corresponding to the initial state $|\psi_0\rangle$.

From figure 1 we note that, when $\delta$ is small, $\widetilde{\lambda}'_0$ and $\widetilde{\lambda}'_1$ are still in the vicinity of 1. This means $\widetilde{U}'$ still has two nearly degenerate states whose eigenvalues are close to 1.

Since the presence of phase noise does not alter the symmetry of the system, we can reduce the perturbed random walk on the hypercube to a walk on the line. Then the operator $\widetilde{U}'$ can be described as

$$\widetilde{U}' = \widetilde{U} - (1-\mathrm{e}^{\mathrm{i}\theta})|L, 1\rangle\langle R, 0|, \tag{13}$$

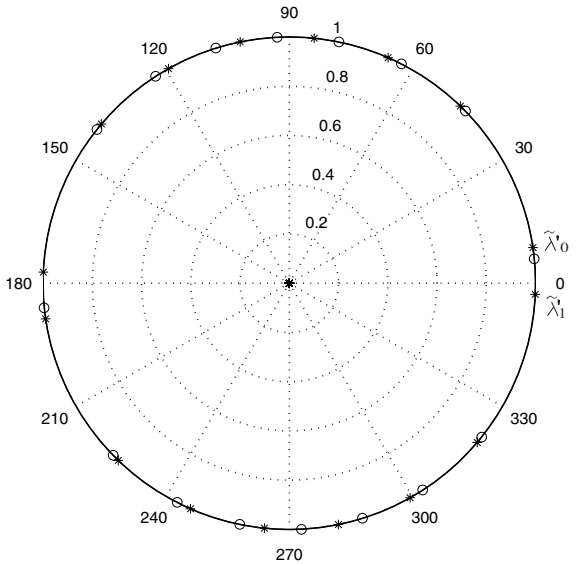


**Figure 1.** The results of numerical spectral analysis of $\widetilde{U}$ and $\widetilde{U}'$ for $n = 8$ with the noise $\delta = 0.1$. The circles indicate eigenvalues of $\widetilde{U}$ while the stars indicate eigenvalues of $\widetilde{U}'$.

where $\widetilde{U}$ is redefined as

$$\begin{aligned}\widetilde{U} = \sum_{x=0}^{n-1} |R,x\rangle \left\{ \left[ \frac{1-\mathrm{e}^{\mathrm{i}\theta}}{n} \sqrt{(x+1)(n-x-1)} \right] \langle R, x+1| \right. \\ \left. + \left[ -1 + \frac{1-\mathrm{e}^{\mathrm{i}\theta}}{n}(x+1) \right] \langle L, x+1| \right\} \\ + \sum_{x=1}^{n} |L,x\rangle \left\{ \left[ -\mathrm{e}^{\mathrm{i}\theta} - \frac{1-\mathrm{e}^{\mathrm{i}\theta}}{n}(x-1) \right] \langle R, x-1| \right. \\ \left. + \left[ \frac{1-\mathrm{e}^{\mathrm{i}\theta}}{n} \sqrt{(x-1)(n-x+1)} \right] \langle L, x-1| \right\}.\end{aligned}$$

The initial state $|\psi_0\rangle$ and the final state $|\psi_1\rangle$ then can be written as [6]

$$|\psi_0\rangle = \frac{1}{\sqrt{2^n}}|R,0\rangle + \frac{1}{\sqrt{2^n}}|L,n\rangle + \sum_{x=1}^{n-1} \left( \sqrt{\frac{\binom{n-1}{x-1}}{2^n}}|L,x\rangle + \sqrt{\frac{\binom{n-1}{x}}{2^n}}|R,x\rangle \right) \tag{14}$$

$$|\psi_1\rangle = \frac{1}{c} \sum_{x=0}^{n/2-1} \left( \sqrt{\frac{1}{2\binom{n-1}{x}}}|R,x\rangle - \sqrt{\frac{1}{2\binom{n-1}{x}}}|L,x+1\rangle \right) \tag{15}$$

where $c$ is a constant which approximately equals 1,

$$c = \sqrt{\sum_{x=0}^{n/2-1} \frac{1}{\binom{n-1}{x}}}.$$

Expanding equation (11) to the second order with respect to $\delta$ (since $\delta \ll 1$) and using the method presented in [6], one can prove that $\widetilde{U}'$ has at most two eigenvalues with their real part greater than $1 - L$, where

$$L = \frac{2}{3n} - \frac{\sqrt{n-1}}{3n}\delta - \left(\frac{1}{6n} - \frac{1}{12}\right)\delta^2. \tag{16}$$

Using equations (13)–(15), one obtains

$$\langle\psi_0|\widetilde{U}'|\psi_0\rangle = \mathrm{e}^{\mathrm{i}\delta} - \frac{(1+\mathrm{e}^{\mathrm{i}\delta})}{2^n}, \tag{17}$$

$$\langle\psi_1|\widetilde{U}'|\psi_1\rangle = 1 - \frac{(1+\mathrm{e}^{\mathrm{i}\delta})}{4c^2\binom{n-1}{n/2}}. \tag{18}$$

From equations (17) and (18), we note that, apart from a small residual, $|\psi_0\rangle$ is 'almost' an eigenvector of $\widetilde{U}'$ with eigenvalue $\mathrm{e}^{\mathrm{i}\delta}$, and $|\psi_1\rangle$ is also 'almost' an eigenvector of $\widetilde{U}'$ with eigenvalue 1. We obtain that, when $\delta^2 \sim 4/2^n$, the rhs of equations (17) and (18) are both close (but not equal) to 1, and hence $|\psi_0\rangle$ and $|\psi_1\rangle$ are nearly degenerate. Then the search algorithm can work normally. A similar result has also been found in the Grover search algorithm in the presence of constant phase noise [20], which suggests that there is a threshold of $\delta \sim 1/\sqrt{N}$ for systematic errors.

We can expand $|\psi_0\rangle$ and $|\psi_1\rangle$ with two eigenvectors of $\widetilde{U}'$, $|\widetilde{\omega}_0'\rangle$ and $|\widetilde{\omega}_1'\rangle$, whose eigenvalues are $\mathrm{e}^{\mathrm{i}\widetilde{\omega}_0'}$ and $\mathrm{e}^{\mathrm{i}\widetilde{\omega}_1'}$. The expansions read

$$\begin{aligned}
|\psi_0\rangle &= C_{00}|\widetilde{\omega}_0'\rangle + C_{01}|\widetilde{\omega}_1'\rangle + \sqrt{1-|C_{00}|^2-|C_{01}|^2}|\gamma_0\rangle,\\
|\psi_1\rangle &= C_{10}|\widetilde{\omega}_0'\rangle + C_{11}|\widetilde{\omega}_1'\rangle + \sqrt{1-|C_{10}|^2-|C_{11}|^2}|\gamma_1\rangle,
\end{aligned} \tag{19}$$

where $C_{00}$, $C_{01}$, $C_{10}$ and $C_{11}$ are four complex coefficients, and they are the functions of $n$ and $\delta$. $|\gamma_0\rangle$ and $|\gamma_1\rangle$ are two normalized vectors orthogonal to $|\widetilde{\omega}_0'\rangle$ and $|\widetilde{\omega}_1'\rangle$. From equations (17)–(19), we obtain

$$(1-\varepsilon_1) \equiv |C_{00}|^2 + |C_{01}|^2 > 1 - \frac{1}{L}\left(\frac{4-\delta^2}{2^{n+1}} + \frac{\delta^2}{2}\right), \tag{20}$$

$$(1-\varepsilon_2) \equiv |C_{10}|^2 + |C_{11}|^2 > 1 - \frac{1}{L}\left(\frac{4-\delta^2}{8c^2\binom{n-1}{n/2}}\right). \tag{21}$$

With the above results, we are able to describe the overall operation of the algorithm. Starting with the initial state $|\psi_0\rangle$, by using equation (19), we can obtain

$$\begin{aligned}
(\widetilde{U}')^t|\psi_0\rangle &= C_{00}\,\mathrm{e}^{\mathrm{i}\widetilde{\omega}_0' t}|\widetilde{\omega}_0'\rangle + C_{01}\,\mathrm{e}^{\mathrm{i}\widetilde{\omega}_1' t}|\widetilde{\omega}_1'\rangle + \sqrt{\varepsilon_1}\left|\gamma_0^t\right\rangle\\
&= P_1|\psi_0\rangle - P_2|\psi_1\rangle - P_1\sqrt{\varepsilon_1}|\gamma_0\rangle + P_2\sqrt{\varepsilon_2}|\gamma_1\rangle + \sqrt{\varepsilon_1}\left|\gamma_0^t\right\rangle,
\end{aligned} \tag{22}$$

where $\left|\gamma_0^t\right\rangle \equiv (\widetilde{U}')^t|\gamma_0\rangle$, and

$$P_1 = \frac{C_{00}C_{11}\,\mathrm{e}^{\mathrm{i}\widetilde{\omega}_0' t} - C_{01}C_{10}\,\mathrm{e}^{\mathrm{i}\widetilde{\omega}_1' t}}{C_{00}C_{11} - C_{01}C_{10}}, \qquad P_2 = \frac{C_{00}C_{01}(\mathrm{e}^{\mathrm{i}\widetilde{\omega}_0' t} - \mathrm{e}^{\mathrm{i}\widetilde{\omega}_1' t})}{C_{00}C_{11} - C_{01}C_{10}}. \tag{23}$$

When $\delta \to 0$, the evolution operator $\widetilde{U}'$ is real, and we obtain $\varepsilon_1, \varepsilon_2 \approx 0$. When $t = t_f$, $P_1$, $P_2 \to 0, 1$, and there will be a high probability of obtaining the state $|\psi_1\rangle$. However, when $\delta \neq 0$, $P_2$ could not reach its maximum $\left(P_2^{\max}\right)$ after $t_f$ iterations, and $P_2^{\max}$ will be much smaller than 1. Since the state $|\psi_1\rangle$ contains a contribution of nearly $1/2$ from the target state, whether the search algorithm is reliable will depend on whether the operator $\widetilde{U}'$ rotates the initial state $|\psi_0\rangle$ to the state $|\psi_1\rangle$. This will finally depend on $\mathrm{e}^{\mathrm{i}\widetilde{\omega}_0'}$, $\mathrm{e}^{\mathrm{i}\widetilde{\omega}_1'}$, and the four coefficients, $C_{00}$, $C_{01}$, $C_{10}$ and $C_{11}$.

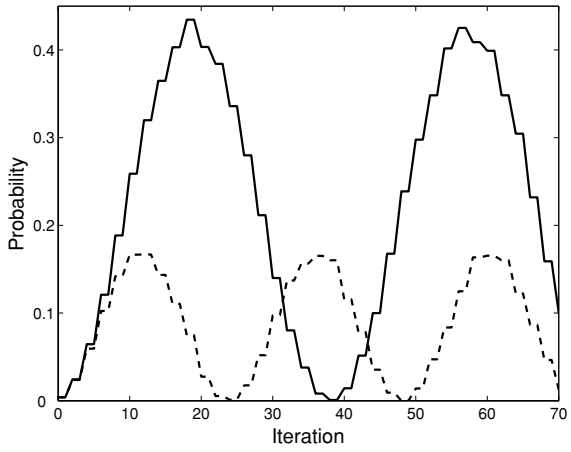


**Figure 2.** The probability of finding the marked state versus the times of iterations when $n = 8$. Solid line for $\delta = 0$, and dashed line for $\delta = 0.2$.

## 4. Numerical simulations

In this section, we will give numerical studies of the QRW search algorithm with phase noise. As we have discussed, if there is phase noise, the probability of finding the marked state will not be able to reach its maximum after $t_f$ iterations. Therefore, the peak of the probability will shift. In figure 2, we compare a case without phase noise ($n = 8$ and $\delta = 0$) and a case in the presence of noise ($\delta = 0.2$). We observe that the probability reaches its peak after 18 iterations for $\delta = 0$, and 12 iterations for $\delta = 0.2$. Thus, due to the presence of the phase noise, the probability of finding the marked state will reach its maximum faster. However, this does not mean that the noisy case is more efficient than the noiseless one, because a drop also occurs in the maximum probability. The above result can also be obtained by equation (23). When $n = 8$ and $\delta = 0.2$, we obtain the eigenvalues $e^{i\tilde{\omega}'_0} = 0.9739 + 0.2268i$ and $e^{i\tilde{\omega}'_1} = 0.9996 + 0.0228i$ by numerical calculations, and find $|P_2|$ reaches its maximum at $t = 12$.

The relationship between the number of iterations needed to reach the maximum probability of the marked state and the size of the database is shown in figure 3. Here we assume that the errors in the phase inversions are systematic, i.e. $\delta$ is constant in each step (model I). The curve of $t_{\max}$ has a transition point at about $n_{\rm cr} \simeq 2(1 - \log_2 \delta)$. An obvious shift can be observed when $n > n_{\rm cr}$. The curve mostly fits for the following formula,

$$t_{\max} = \frac{\pi}{\sqrt{8/N + \delta^2}}, \tag{24}$$

where $N = 2^n$ is the size of database. Next we study the relationship between the maximum success rate and the size of the database for model I. We vary $n = \log_2 N$ and run the algorithm with a sufficient number of iterations so that a maximum probability is found. Our numerical results show that the phase noise results in a reduction in the maximum probability of finding the marked state, as shown in figure 4. When $n$ is large, the probability decreases exponentially. This result shows that, due to the phase error, the database size cannot be unlimited. From the figure, we note that there is still a transition point in each curve which is determined by the error parameter $\delta$. The curve of the probability mostly fits for the following form,

$$P_{\max} = \frac{8P_0}{8 + \delta^2 N}, \tag{25}$$

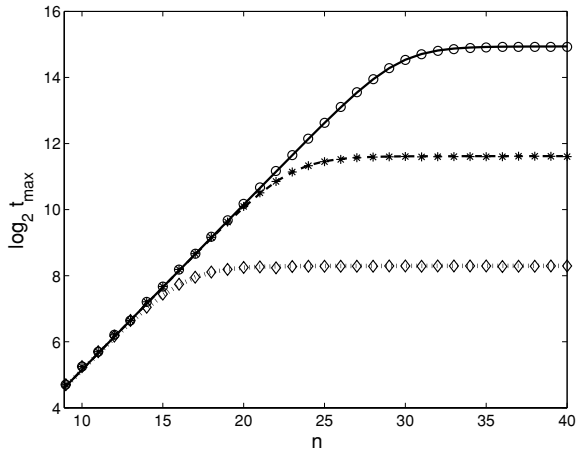


**Figure 3.** The number of iterations required to reach the maximum probability versus $n = \log_2 N$ for model I, where only systematic errors in the phase inversions are counted. Diamonds are used for $\delta = 0.01$, asterisks for $\delta = 0.001$, and circles for $\delta = 0.0001$. The dotted, dashed and solid curves fitting for the numerical data are obtained by equation (24).

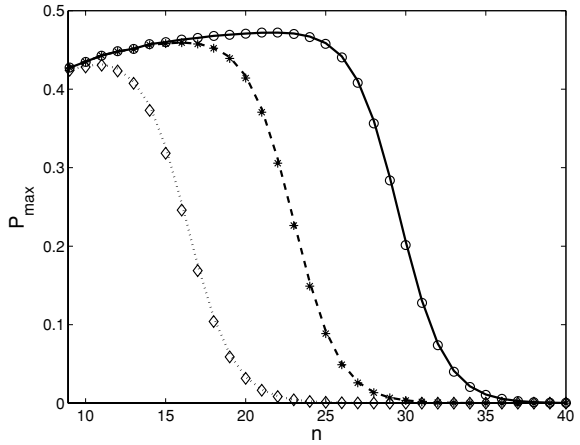


**Figure 4.** The maximum probability of finding the marked state versus $n = \log_2 N$ for model I. Diamonds are used for $\delta = 0.01$, asterisks for $\delta = 0.001$ and circles for $\delta = 0.0001$. The dotted, dashed and solid curves fitting for the numerical data are obtained by equation (25).

where $P_0$ is the probability of finding the marked state in the noiseless case. Equation (25) shows, if $N \to \infty$, the QRW search algorithm is available only when $\delta = 0$. Equations (24) and (25) provide analogies between the QRW search algorithm and the Grover search algorithm, both of which show the algorithmic success probability dropped dramatically under the condition $\delta > 1/\sqrt{N}$ in the presence of systematic errors [20].

In experiments, there are systematic errors as well as random errors, and we cannot estimate them precisely. One may still run the algorithm for $t_f$ iterations when the Grover diffusion operator is used. However, the probability of finding the target state will not reach its maximum when a measurement is taken at $t_f$. We study the variation of the probability with increasing of noise under the condition $t = t_f$ (where $t_f$ is defined in equation (5)). We simulate the case of $n = 6, 7, 8$, i.e. the size of database is $N = 64, 128, 256$ for the model I (as shown in figure 5) and another two error models (as shown in figures 6 and 7). The second

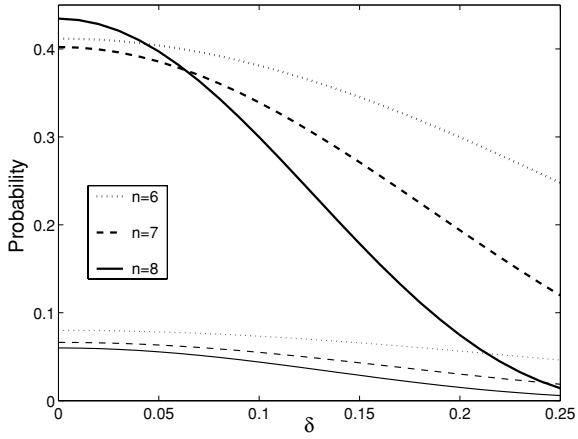


**Figure 5.** Upper three traces, the probability of finding the marked state versus $\delta$ for model I, where only systematic errors are counted. Lower three traces, the highest probability of the rest states versus $\delta$ with the same legend.

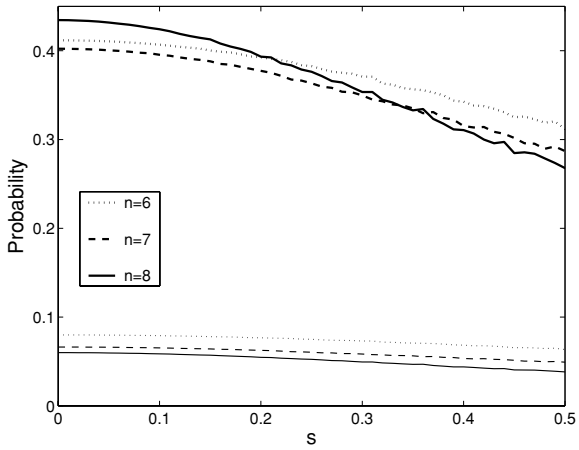


**Figure 6.** The probability of finding the marked state versus the standard deviation $s$ for model II, where only random errors are counted. The mean of the noise $\delta_0 = 0$.

error model assumes that $\delta$ in each step is a Gaussian random variable with mean $\delta_0 = 0$ and standard deviation $s$ (model II). It is conventionally defined as *random* error. Finally, we let $\delta$ be a Gaussian random variable with mean $\delta_0 \neq 0$ and standard deviation $s$ (model III). Each curve in figures 6 and 7 is the average over 200 simulations for each point because of the randomness of the phase errors. Figures 5 and 6 show that the systematic errors play a more significant role than the random errors. The numerical results also show that the mean success rate for model II $\sim O(1/s^2\sqrt{N})$ (when $N \gg 1$), which confirms the analysis of [20] and [21] regarding the success rate with random errors in the Grover search algorithm. The probability in figure 7 is nearly identical to that in figure 5 except for some small fluctuations. The reason is that the effects of random errors will counteract each other during the application of operator $\widetilde{U}'$ while the effects of the systematic errors will accumulate.

Next we study the gap which is defined as the distance between the probability of the target state and the highest probability of the rest states. Although the probability of the target

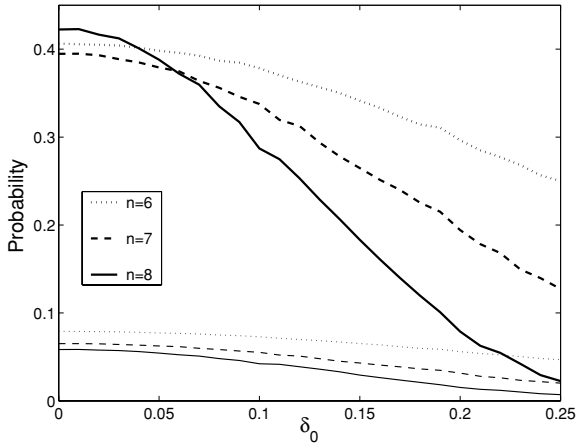


**Figure 7.** The probability of finding the marked state versus noise for model III, where both random and systematic errors are counted. $s = 0.1$, $\delta_0 = 0, \ldots, 0.25$.

state is useful, the ability to distinguish the target state from others is also important. In relevant experiments such as NMR, the final state is not determined directly. An equivalent measurement, so-called quantum state tomography [15], is made to recover the density matrix $\rho(t) = |\psi_1(t)\rangle\langle\psi_1(t)|$. The diagonal elements of the final density operator are obtained and the off-diagonal elements can be cancelled by applying gradient pulse before readout pulse when we use heteronuclear systems. After repeating the algorithm around $t_f$ times, one may find that the probability of finding the target state is much higher than others. This means, if the gap is large enough, we may say that the search is still successful in view of experiment. When $n = 8$, the gap decreases from 0.3745 to 0.0083 as $\delta$ varies from 0 to 0.25 (as shown in figure 5), while the marked state probability decreases from 0.4345 to 0.0141. The gap decreases slower than the probability of finding the target state.

Finally, we draw a comparison between the QRW search algorithm and the Grover search algorithm. The maximum probabilities in both algorithms drop exponentially with the increasing size of database in response to the systematic errors, while the random errors do not affect the algorithm as significantly as the systematic errors. In [20, 21], it was shown that there is a threshold of $\delta \sim 1/N^{1/2}$ for systematic errors and $s \sim 1/N^{1/4}$ for random errors. In our simulations results, the QRW search algorithm exhibits a similar behaviour as the Grover search algorithm. However, as presented in [6], the coin operator in the QRW acts only on the $n$-dimensional coin space, and all our operations in an iteration are $n$ local. So the errors introduced in the Grover diffusion operator affect these two algorithms differently. One example is that the phase noise in the Grover search algorithm, as shown in [20], will make the probabilities of all unmarked states rise and the probability of the marked state decrease. However, in the QRW search algorithm, only the probabilities of the nodes which are not adjacent to the marked node will rise, while those of the marked node and adjacent nodes will decrease. This is why figures 5–7 show that the highest probability on the unmarked nodes will also decrease with increasing error.

## 5. Conclusions

In this paper, we have studied how imperfect quantum gates affect the QRW search algorithm. Our model assumed that there is a phase noise in the Grover diffusion operator. We find, from

our analysis, that such a noise will not only reduce the maximum probability of finding the marked state, but also shift the peak position, which has also been shown in our numerical results. The maximum probability of the target state relies on the size of database and the errors as revealed in equation (25). Numerical studies also indicate that random errors in the phase inversion do not affect the algorithm as seriously as the systematic errors. Thus, in practice more attention should be paid to reduce the systematic errors.

However, the phase errors still occur inevitably due to imperfection in experiments. For instance, systematic errors arise from inhomogeneity in radio frequency pulses in NMR realizations. And random errors may originate from fluctuations of the laser intensities and detunings in EIT realizations [23]. These errors will affect the reliability of the algorithm. It is necessary to make an estimate of the combined effect of systematic errors and random errors and set an upper bound for the size of a quantum database to ensure the success rate.

As a final comment, we point out that unlike the Grover search algorithm, the phase noise in the Grover diffusion operator in the QRW search algorithm does not make the probabilities on all unmarked nodes rise. It is not clear whether other coins or kinds of noises will have the same properties. This might be a valuable direction for future works.

## Acknowledgment

The work was supported by National Fundamental Research Program grant no. 2001CB309300 of People's Republic of China.

## References

[1] Grover L K 1997 *Phys. Rev. Lett.* **79** 325
[2] Yamaguchi F, Milman P, Brune M, Raimond J M and Haroche S 2002 *Phys. Rev.* A **66** 010302
[3] Jones J A, Mosca M and Hansen R H 1998 *Nature* **393** 344
[4] Chuang I L, Gershenfeld N and Kubinec M 1998 *Phys. Rev. Lett.* **80** 3408
[5] Zubairy M S, Matsko A B and Scully M O 2002 *Phys. Rev.* A **65** 043804
[6] Shenvi N, Kempe J and Whaley K B 2003 *Phys. Rev.* A **67** 052307
[7] Childs A M and Goldstone J 2004 *Phys. Rev.* A **70** 022314
[8] Ambainis A 2003 *Preprint* quant-ph/0311001
[9] Aharonov Y, Davidovich L and Zagury N 1993 *Phys. Rev.* A **48** 1687
[10] Farhi E and Gutmann S 1998 *Phys. Rev.* A **58** 915
[11] Ambainis A, Bach E, Nayak A, Vishwanath A and Watrous J 2001 *Proc. 30th Annual ACM Symposium on Theory of Computing (STOC)* (New York: ACM) pp 60–9
[12] Childs A M, Farhi E and Gutmann S 2002 *Quantum Inf. Process* **1** 35
[13] Kempe J 2002 *Preprint* quant-ph/0205083
[14] Travaglione B C and Milburn G J 2002 *Phys. Rev.* A **65** 032310
[15] Du J F *et al* 2003 *Phys. Rev.* A **67** 042316
[16] Chuang I L, Laflamme R, Shor P W and Zurek W H 1995 *Science* **270** 1633
[17] Preskill J 1998 *Proc. R. Soc.* A **454** 385
[18] Kendon V and Tregenna B 2003 *Phys. Rev.* A **67** 042315
Kendon V and Tregenna B 2003 *Preprint* quant-ph/0301182
[19] Russell G and Alagic A 2005 *Phys. Rev.* A **72** 062304
[20] Long G L, Li Y S, Zhang W L and Tu C C 2000 *Phys. Rev.* A **61** 042305
[21] Shenvi N, Brown K R and Whaleyf K B 2003 *Phys. Rev.* A **68** 052313
[22] Moore C and Russellf A 2001 *Preprint* quant-ph/0104137
[23] Ottavianif C *et al* 2003 *Phys. Rev. Lett.* **90** 197902
Rebić S *et al* 2004 *Phys. Rev.* A **70** 032317